Hydrolysis of $SnCl_2$ on Polyaniline: Formation of Conducting PAni-SnO_2 Composite with Enhanced Electrochemical Properties

Chepuri R. K. Rao,[1*] M. Vijayan,[2] Shahid Anwar,[3] D. Jeyakumar[2]

[1]*Organic Coatings and Polymers Division, Indian Institute of Chemical Technology, Hyderabad 500 007, India*
[2]*Functional Materials Division, Central Electrochemical Research Institute, Karaikudi 630006, India*
[3]*Central Instrumental Facility, Central Electrochemical Research Institute, Karaikudi 630006, India*

Received 5 May 2011; accepted 2 September 2011
DOI 10.1002/app.35587
Published online 6 December 2011 in Wiley Online Library (wileyonlinelibrary.com).

ABSTRACT: First time in the literature, we report that polyaniline-EB can be doped by $SnCl_2$ to give conducting SnO_2 doped polyaniline novel material. The composite is characterized by Fourier transform infrared, ultraviolet-visible, X-ray diffraction, scanning electron micrograph, transmission electron microscopy, and electrochemical methods. The new composite exhibited improved electrochemical properties compared with the virgin polymer. The composite is also expected for its high sensitivity for recognizing volatile organic compounds. © 2011 Wiley Periodicals, Inc. J Appl Polym Sci 124: 4819–4826, 2012

Key words: tin chloride; polyaniline; tin oxide; doping; specific capacitance

INTRODUCTION

Polyaniline (PAni) is regarded as one of the potentially attractive conducting polymers because of its tunable conductivity by controlled doping, easy formation of processable fibers, and commercial viability.[1–3] The applications of the electrochemically active conducting PAni as a bulk material or nanofibers is well documented and still found increasing.[4–8] Nanostructured PAni, for example, nanofibers, are more responsive than bulk PAni to external stimulation due to their large surface area, and hence, they are identified as promising materials in sensing and catalytic applications.[7,9,10] PAni-metal composites exhibit broadened applications such as sensing and electrocatalysis, compared with pure PAni.[11–14] The mechanism involved in doping of PAni-EB (polyaniline-emeraldine base form) into conducting PAni salt is interesting and is restricted to strong acids with low pK_a values. Doping of PAni-EB with other materials is challenging and paves the way for fabricate useful PAni composites.[15,16]

Tin oxide (SnO_2) is a typical wide band gap *n*-type semiconductor with $E_g = 3.6$ eV at room temperature and has applications such as in lithium ion batteries, solar cells, catalysis, and gas sensing and supercapacitor electrode materials.[17–24] In recent times, the research on SnO_2 is mostly focused on gas sensing applications with SnO_2 material in nanodimensions,[25] the other usage of this material being as battery or capacitor with particular attention on SnO_2/graphite or SnO_2/carbon nanotubes (CNTs) composites.[18] There are only few reports available on the synthesis of SnO_2 composites with conducting polymer.[26–33] Kulszewicz-Bajer et al. studied the doping effects of Lewis acids such as $FeCl_3$ and $SnCl_4$ on PAni-EB material. These authors found that PAni can be solubilized in nitromethane via complexation with $SnCl_4$ and forms free-standing film.[27] Recently, PAni/SnO_2 composites useful for ammonia gas sensing[29,30] or other volatile organic compound (VOC) sensors[31] have been also reported in literature. Some PAni/SnO_2 composites exhibiting useful nonlinear optical[32] properties and electrochromic display[33] properties were also reported.

In our continued efforts to synthesize novel conducting polymer-metal(oxide) composites[34–38] [CP-M(O)], we focused on PAni/SnO_2 composites believing that these composites exhibit improved electrochemical properties. The aim of the article is to synthesize SnO_2 doped polyaniline (PAni-SnO_2) composite, in a novel and unprecedented way, using $SnCl_2$ and presynthesized PAni-EB as precursors and evaluate its use. The composite is expected to show potential applications: first, as tinoxide is one of the attractive oxide materials for supercapacitor electrode material,[24] the composite PAni-SnO_2 would be a favorable choice to enhance the capacitance. Second, as both PAni[5] and tin oxide are known to be good gas/VOC sensor materials,[25] the composite material work more efficiently. In this

Correspondence to: C. R. K. Rao (ramchepuri@iict.res.in).

communication, we describe our results on the doping effects of tin chloride on PAni and the electrochemical properties of the composites.

EXPERIMENTAL

All chemicals are analytical grade. Aniline and tin dichloride were obtained from MERCK Chemicals (India). $SnCl_2.2H_2O$ is purchased from CDH (India) Chemicals. Polyvinylidenefluoride (PVDF) and Nafion (5%) solutions were purchased from Aldrich Chemical Company (USA).

Fourier transform infrared (FTIR) spectra of the samples were recorded on model no. nexus-670 spectrometer from Thermonicolet. Scanning electron micrograph (SEM) images were taken on Hitachi 3000 H instrument. X-ray diffraction (XRD) experiments were conducted on PANalytical's X'Pert PRO instrument. Electrochemical experiments such as cyclic voltammetry and charge-discharge behavior were performed on AUTOLAB 302 potentiostat using three electrode assembly containing platinum disc working electrode (2 mm diameter), platinum wire auxiliary electrode, and saturated calomel reference electrode (S.C.E.). For cyclic voltammetry, 2.0 mg of the samples were well dispersed in the mixture of 0.8 mL water and 0.2 mL of 5% Nafion solution and 10 uL of this solution was loaded on the Pt electrode and dried at room temperature (R.T.) For charge-discharge experiments, the electrodes were prepared by applying a homogeneous paste [on two sides of a Pt foil of 1.2 cm $\times$ 0.8 cm area] obtained by mixing the composite (80%), carbon 10% (blackpearl), and the binder PVDF(10%) thoroughly in a mortar using *N*-methylpyrrolidone (NMP) as solvent. The dried composite electrode was weighed and used.

Synthesis of PAni-SnO_2 composite through PAni-EB route (composite A)

In a typical synthesis, PAni-EB (microparticles/or nanofibrils, 0.1815 g, 0.5×10^{-3} mol dm^{-3}) in 100 mL of milliQ water was sonicated for 15 min for well dispersion. To this, was mixed $SnCl_2.2H_2O$ dispersion (0.113 g, 5×10^{-4} mol dm^{-3}, well dispersed in 70 mL water) and stirred for 18–24 h. The resultant green-black material was collected by centrifuge, washed with water, and dried at room temperature. The thermogravimetric (TG) analysis showed that 13.1 wt % SnO_2 was deposited on to the PAni.

Synthesis of PAni-SnO_2 composite through *in situ* route (composite B)

In this method, tin oxide is incorporated into polymer by an *in situ oxidation* mechanism. First, anilinium hydrochloride (0.77 g, 6×10^{-3} mol dm^{-3}) and $SnCl_2.2H_2O$ (0.675 g, 3×10^{-3} mol dm^{-3}) were mixed and stirred in water (100 mL) containing 0.7 mL HCl for about 10 h. Then, the mixture was polymerized at room temperature adding ammonium persulphate solution (1.5 g, 6.57×10^{-3} mol dm^{-3}, 50 mL) drop wise for 20 min. The mixture was further stirred for 6 h at room temperature. The blue-green composite was filtered and washed with copious amounts of water and dried at room temperature. TG analysis of the material showed that 29.1 wt % of SnO_2 is present in the composite.

RESULTS AND DISCUSSION

Synthesis and spectral characterization of the composites

We observed that $SnCl_2$ reacts with PAni-EB to give PAni-SnO_2 composite material. The possible mechanism of formation of the SnO_2 is decomposition of $SnCl_2$ in presence of water and oxygen to give HCl and SnO_2. The formed HCl doped PAni-EB while SnO_2 is deposited on PAni particles concomitantly giving PAni- SnO_2 conducting composite as shown in the eqs. (1) and (2)

$$2\,SnCl_2 + 2H_2O + O_2 \rightarrow 2SnO_2 + 4HCl \quad (1)$$

$$[PAni]_{EB} + HCl \rightarrow [PAniH^+ \cdot Cl]_{salt} \quad (2)$$

FTIR spectrum of the composites A and B (Fig. 1) showed bands due to aromatic ring breathing mode in the region 1600–1400 cm^{-1}. Band at 1495 cm^{-1} is the characteristic band assigned to (benzenoid) N-B-N and the band at 1580.7 cm^{-1} is due to nitrogen quinoid (N=Q=N) in pure PAni-EB. The C—N stretching is observed[39–42] at 1302.8 cm^{-1}. After reaction with $SnCl_2$, PAni-EB is partially doped and N-B-N stretching frequency shifted to 1485 cm^{-1}, whereas N=Q=N band shifted to 1568 cm^{-1}. For the *in situ* formed composite B, these bands occur at 1483.6 cm^{-1} and 1561.7 cm^{-1}, respectively. The C—N stretching is seen at 1291.9 and 1299.1 cm^{-1} for A and B composites. Ultraviolet-visible absorption spectra of the as synthesized polyaniline nanofibers in NMP solution displays two absorption bands. The peaks at 327 and 614 nm are related to π-π^* transition of the benzenoid ring and the benzenoid-to-quinoid excitonic transition, respectively, in the polymer chain.[43] The composites A and B show similar absorption bands with shifting of π-π^* transition to 368 nm and benzenoid-to-quinoid excitonic transition occurring at 614 nm; the red shift is attributable to the change in the concentration of benzenoid units after doping.

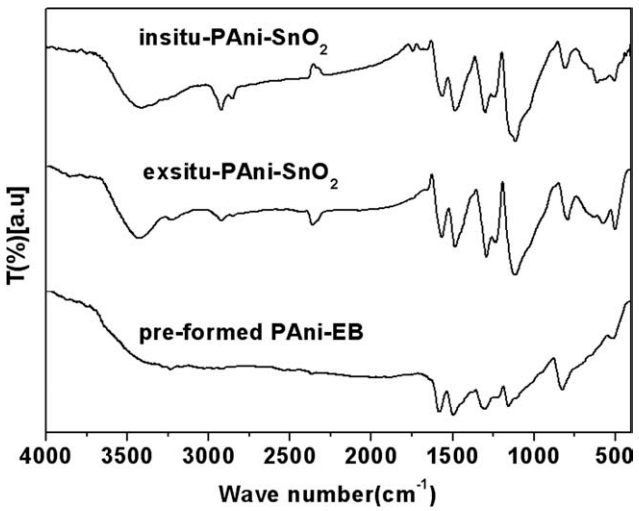

Figure 1 FTIR spectra of the pure PAni-EB and composites A and B.

XRD, thermal and X-ray photoelectron spectroscopic studies

The evidence of formation of SnO_2 can be deduced from XRD profile. Figure 2 shows the XRD profile of the composite. Inset of Figure 2 shows two broad peaks centered at $2\theta = 20$ and 26, which show that the starting material PAni-EB nanostructures are amorphous. The peak centered at $2\theta = 20$ is ascribed to periodicity parallel to the polymer chain, while the latter peaks may be caused by the periodicity perpendicular to the polymer chain.[44] The diffraction peaks of the composites A and B are consistent with the known tetragonal SnO_2 (t-SnO_2).[45] Broad diffractions are observed at $2\theta = 26.6499$ (d-spacing = 3.345 Å), 35.035 (d-spacing = 2.561 Å), 52.258 (d-spacing = 1.7505 Å), and 64.530 (d-spacing =1.444 Å), which correspond to (110), (101), (211), and (112) reflections of t-SnO_2, respectively. X-ray photoelectron spectroscopic (XPS) investigation on the composite further established the presence of SnO_2. Typical narrow-scan analysis of Sn 3d spectra, within the binding energy (B.E) range of 475–505 eV, is presented in Figure 2. The spectrum exhibited a doublet assignable to Sn $3d_{5/2}$ and Sn $3d_{3/2}$ at 486.95 eV and 495.4 eV is observed indicating Sn in (IV) oxidation state.[46]

TG analysis of the material showed that 13.1 wt % of SnO_2 is present in the composite A and 29.1 wt % in composite B. Figure 3 shows TGA curves for pure PAni-EB and composite A (dedoped form). There is a moisture loss of about 8% and 11% in pure PAni-EB and composite A, respectively, which took place about 100°C. The degradation of the polymer starts nearly at 350°C and continues to 615–630°C, and there is no loss of weight incurred after this temperature. The difference in residual weights of PAni and composite A gave the wt % of the SnO_2 present in the composite A, which is 13.1% (Fig. 3). Similar analysis on composite B gave a SnO_2 loading of 29.1 wt %.

Scanning electron microscopy and transmission electron microscopy studies

Figure 4 shows the SEM of the composites A and B. The composite A is porous [Fig. 4(a,b)] and is composed of large size fibrils, typically with diameter $\sim$ 100 nm and length of >200 nm. The composite B is also porous, but the polymer formed a dense net work of fibrils/fibers with diameter of about 100 nm

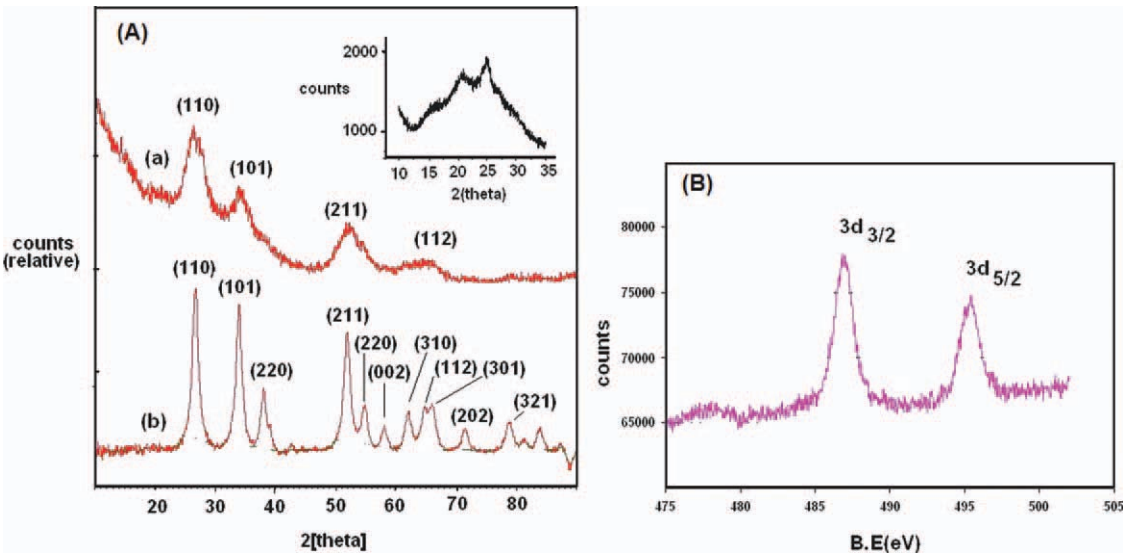

Figure 2 (A) XRD profiles of (a) composite A (b) composite A, after heating at 650°C. Inset shows the XRD of PAni-EB (B) XPS spectrum of the composite A [Color figure can be viewed in the online issue, which is available at wileyonlinelibrary.com].

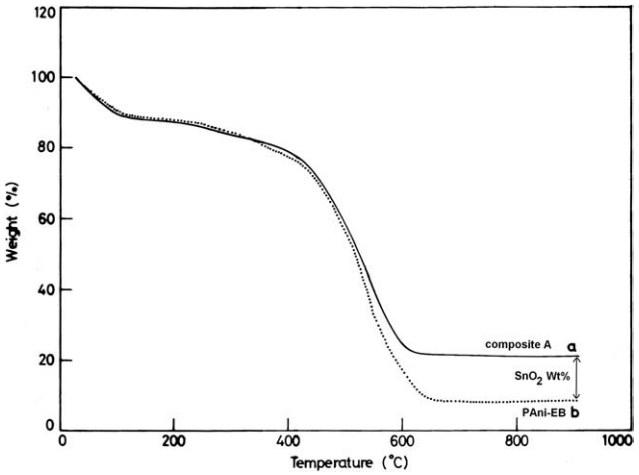

Figure 3 TGA curves for (a) composite A(dedoped form) and (b) PAni-EB.

and length of about 1 μm [Fig. 4(c,d)]. The room temperature electronic conductivity, measured by four-probe method, of the preformed PAni-EB increased to 2.26×10^{-2} S cm^{-1} from insulating regime after reaction with $SnCl_2$. The composite B showed a conductivity of 1×10^{-2} S cm^{-1}. The higher value of conductivity for the composite A is believed to be due to the surface-located SnO_2 particles, which is not the case for composite B.

The two composites A and B were probed by tunneling electron microscopy (TEM) techniques. TEM picture of composite A shows that SnO_2 nanoparticles which are well below 10 nm, were deposited on the microparticles/or nanofibrils of PAni [Fig. 5(a–c)]. The selected area electron diffraction (SAED) picture of the sample is also shown in Figure 5(c). The three polycrystalline rings correspond to crystal faces of (110), (101), and (200) of tetragonal-SnO_2 can be readily identified. The pictures show that SnO_2 particles are deposited all over the fibrils. However, on some fibrils, the deposition of SnO_2 particles is more. This may be due to irregular shapes of fibrils. When the fibril is more uniform, the deposition is more uniform.

The composite B was also analyzed by TEM facility. Figure 5(d–f) shows that SnO_2 nanoparticles of the order of 5–10 nm are deposited on the polymer. TEM analysis also suggests that there are some

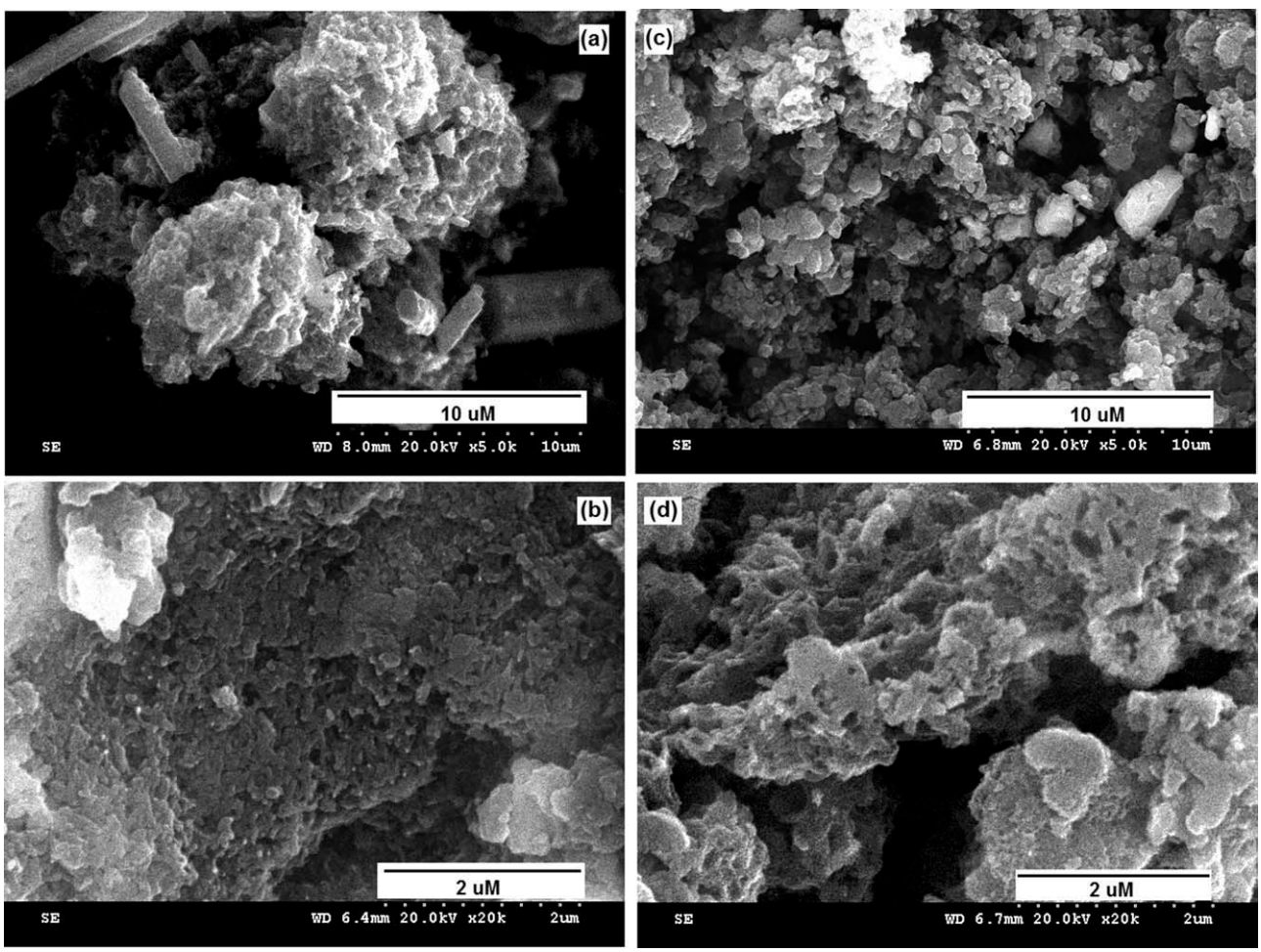

Figure 4 SEMs of composite A (a,b) and B (c,d).

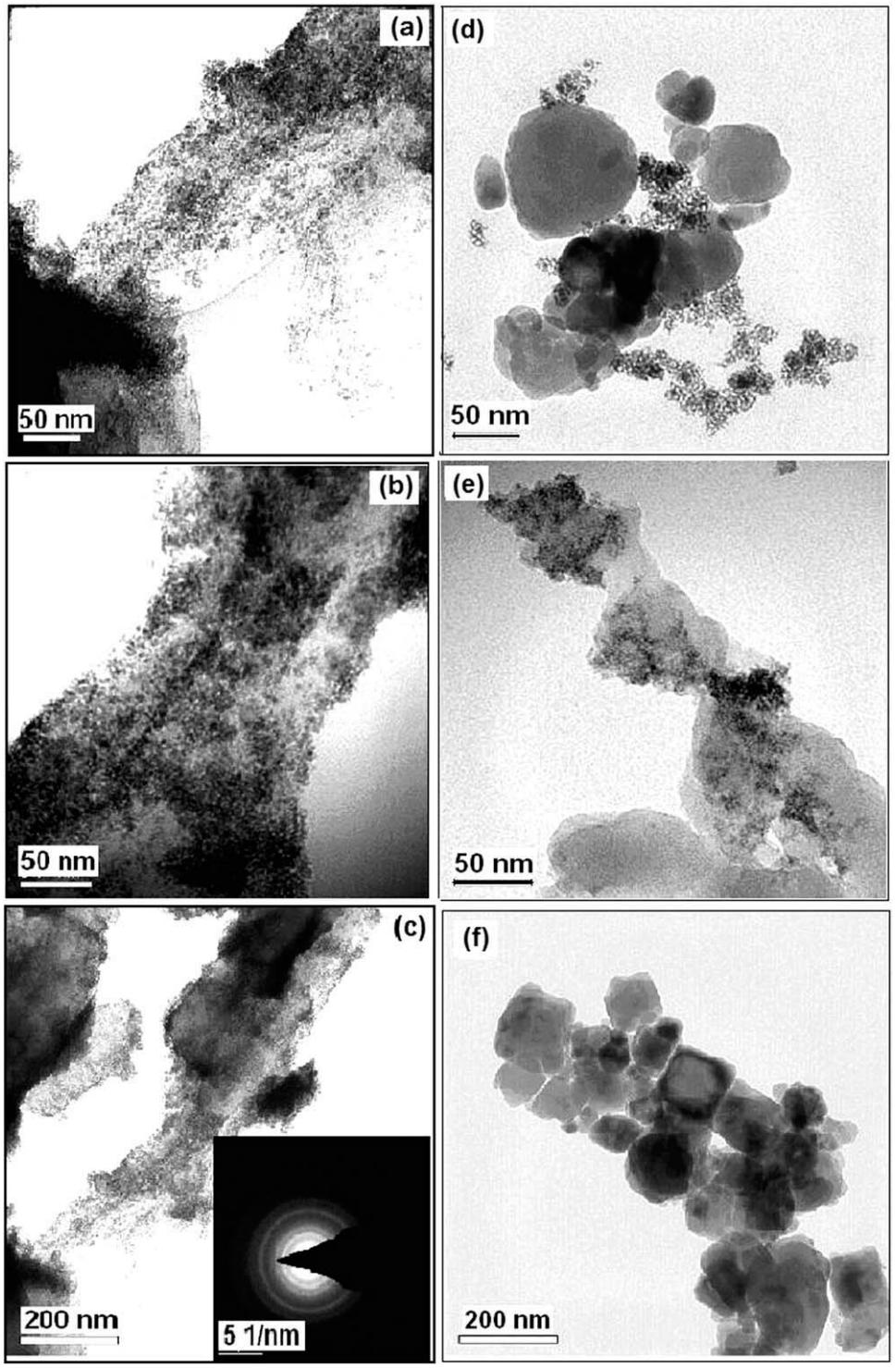

Figure 5 TEM of composite A (a,b,c) and composite B (d,e,f).

PAni particles present [Fig. 5(d)], which were not deposited by SnO_2 particles. This may be due to the assumption that these polymer particles would have been formed after SnO_2 deposition. Overall, the main difference of this sample B with composite A is that SnO_2 particles are not deposited evenly on PAni. In this reaction, PAni is formed in various shapes such as fibrils and round particles [Fig. 5(d,e)]. Some parts of the composite are rich with cube shaped SnO_2 particles [Fig. 5(f)]. This is due to the fact that polymerization of aniline and oxidation of $SnCl_2$ took place simultaneously and independently as soon as oxidizing agent is added. There is no preformed polymer present in the initial stages of conversion of $SnCl_2$ to SnO_2 particles.

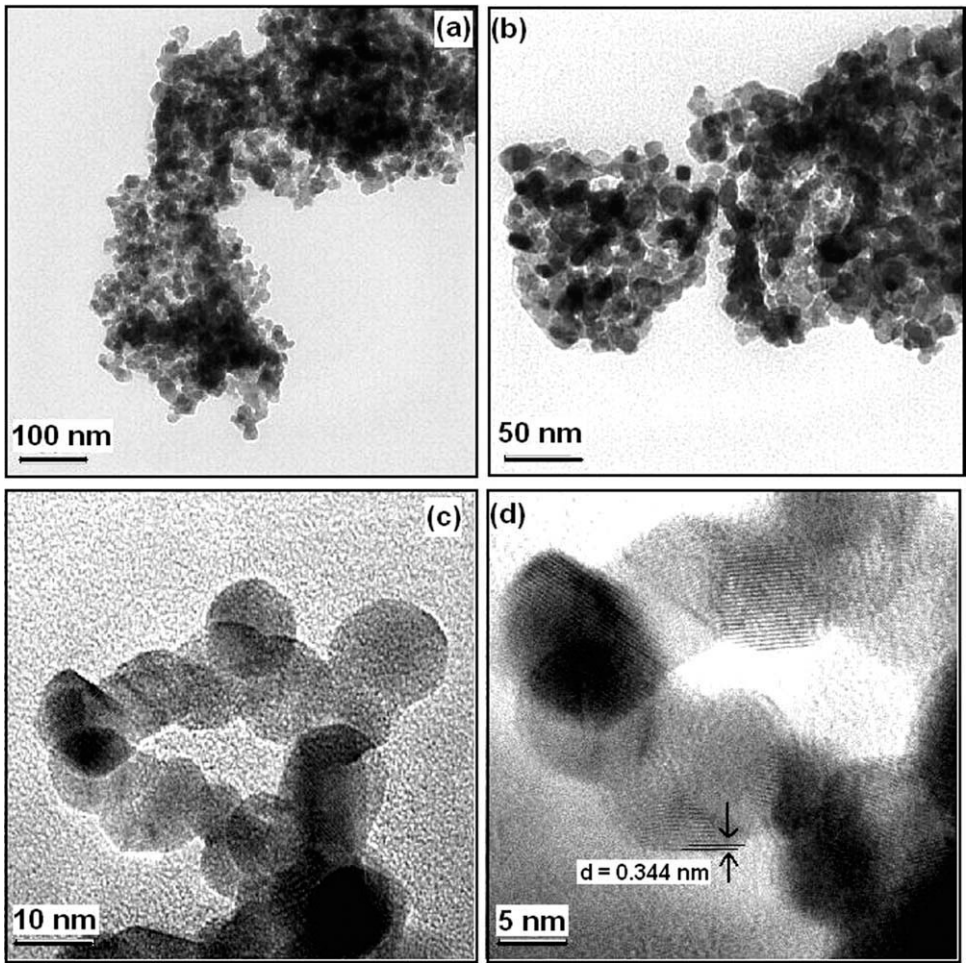

Figure 6 TEM of composite A after heat treatment.

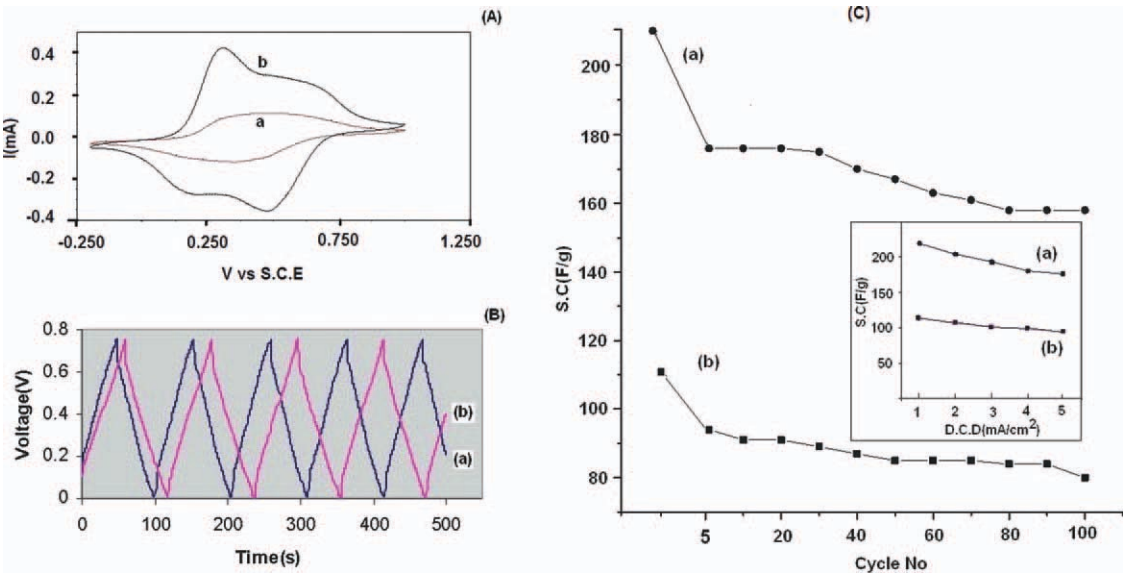

Figure 7 (Part-A) Cyclic voltammetry of the composite B in 1*M* perchloric acid at scan rate of 50 mV s^{-1}(curve b) and pure PAni (curve a). (Part-B) charge-discharge profiles for (a) pure PAni and (b) composite B in 1*M* perchloric acid at a current density of 1 mA cm^{-2}. (Part C) variation of SC values for (a) composite B and (b) pure PAni. Inset shows the dependence of SC with d.c.d. [Color figure can be viewed in the online issue, which is available at wileyonlinelibrary.com].

SnO_2 nanotubes have been prepared with CNTs as template material in the literature.[25] CNTs were later removed by heating the SnO_2/CNT composite. We thought that PAni fibrils can be useful as template to synthesize SnO_2 nanostructures. Hence, composite A was heated to 650°C to remove PAni base material, and the white product was analyzed by XRD and TEM technique. XRD profile [Fig. 2(b)] of the heated sample showed reflections due to (110), (101), (220), (211), (220), (002), (310), (112), (301), (202), and (321) according to JCPDS No 41-1445.[47] These peaks are very sharp and intense in nature which is due to improved crystallization and sintering of the small nanoparticles into bigger clusters. The TEM study showed that only nanosized SnO_2 particles formed as clusters but are not transformed into nanotubes (Fig. 6). This is due to the large size of the PAni fibrils, which were only worked as base material but not as a templating fiber. The *d*-spacing of SnO_2 nanparticles, shown in Figure 6, is 0.334 nm corresponding to the (110) face of *t*-SnO_2.

Electrochemical properties

The composites A, B and PAni-SnO_2 were tested for its electrochemical activity vis-à-vis with the pure PAni. The study showed that the composite B is more electrochemically active than A and pure PAni and hence can be a useful as material for electrochemical capacitor. Figure 7(A) shows cyclic voltammogram (CV) of the composite B and PAni prepared under same experimental conditions. Figure 7(A) clearly shows that the composite gave nearly four times higher current density (b) compared with the virgin polymer (a).

From the CV behavior, it is expected that the composite material is useful for supercapacitor electrode material. For this purpose, composite electrodes of B with Pt foil as current collector were prepared as described in the experimental section. The electrodes were subjected to charge–discharge tests [Fig. 7(B)] from 0.0 to 0.75 V in 1*M* perchloric acid, and the specific capacitance (SC) values were calculated from discharge times using the formula $SC = It/0.75$ m, where I = current density, t = discharge time (in seconds), and m = mass of the electroactive material. Inset in Figure 7(c) shows that when the discharge current density (d.c.d.) is varied between 1 and 5 mA cm^{-2}, the SC value of the composite varied between 219 and 176 F g^{-1}. Figure 7(B) shows typical charge–discharge profile of the composite (a) compared with pure PAni (b).The composite at a d.c.d. of 1 mA cm^{-2} exhibited a SC of 219 F g^{-1} which fall to 158 F g^{-1} in 100 cycles, whereas the pure PAni showed the value in the range 113–80 F g^{-1} [Fig. 7(c)]. This indicates that the composite is useful as electrode material for the supercapacitor.

The possible future application of the nanocomposite is sensing toxic VOCs such as methanol or chloroform vapors. It is believed that when the active sensing material SnO_2 is deposited on PAni heterogeneously similar to composite A (rather than SnO_2 incorporated homogeneously in the second composite B), the sensing property of the composite will be increased due to synergistic effect. Experiments are in progress in this direction in our laboratory to establish these effects of having SnO_2 on the surface of the PAni fibers, which are already known to be excellent gas sensor materials.[5]

SUMMARY

In conclusion, first time we report that $SnCl_2$ can dope PAni-EB form by producing SnO_2 and HCl. The formed HCl doped the quinoid segments of the E.B structure in a conventional way to form conducting PAni salt and SnO_2 is deposited on the surface of the polymer concomitantly to give conducting PAni-SnO_2 composite. In this method of preparation (composite A), tin oxide particles are deposited on PAni fibers. In the case of *in situ* polymerization (composite B), the composite is a homogeneous mixture of some free SnO_2 particles, SnO_2 on PAni and as well as SnO_2 encapsulated/embedded in PAni. The conductivity of the samples A and B increased significantly due to the presence of SnO_2 nanoparticles, where the tin oxide particles are crystallized in tetragonal (*t*-SnO_2) structure. In this study, it is also established that composite A and B exhibited improved electrochemical property compared with pure PAni. The composite B showed enhanced pseudo capacitance as high as 219 F g^{-1}.

The authors thank the directors of IICT and CECRI for their constant encouragement, unstinted support.

References

1. Skotheim, T. A.; Elsenbaumer, R. L.; Reynolds, J. R., Eds. Handbook of Conducting Polymers, 2nd ed.; Marcel Dekker: New York, 1997.
2. Huang, J.; Virji, S.; Weiller, B. H.; Kaner, R. B. J Am Chem Soc 2003, 125, 314.
3. Huang, J.; Kaner, R. B. J Am Chem Soc 2004, 126, 851.
4. Novak, P.; Muller, K.; Santhanam, K. S. V.; Haas, O. Chem Rev 1997, 97, 207.
5. Li, D.; Huang, J.; Kaner, R. B. Acc Chem Res 2009, 42, 135.
6. Virji, S.; Kaner, R. B.; Weiller, B. H. J Phys Chem B 2006, 110, 22266.
7. Virji, S.; Huang, J.; Kaner, R. B.; Weiller, B. H. Nano Lett 2004, 4, 491.
8. Virji, S.; Kojima, R.; Fowler, J. D.; Kaner, R. B.; Weiller, B. H. Chem Mater 2009, 21, 3056.
9. Kanungo, M.; Kumar, A.; Contractor, A. Q. Anal Chem 2003, 75, 5673.

10. Janata, J.; Josowicz, M. Nat Mater 2003, 2, 19.
11. Kitani, A.; Akashi, T.; Sugimoto, K.; Ito, S. Synthetic Met 2001, 121, 1301.
12. Kinyanjui, J. M.; Hatchett, D. W.; Anthony Smith, J.; Josowicz, M. Chem Mater 2004, 16, 3390.
13. Sarma, T. K.; Chattopadhyay, A. Langmuir 2004, 20, 4733.
14. Pillalamarri, S. K.; Blum, F. D.; Tokuhiro, A. T.; Bertino, M. F. Chem Mater 2005, 17, 5941.
15. Ryu, K. S.; Jeong, S. K.; Joo, J.; Kim, K. M. J Phys Chem B 2007, 111, 731.
16. Ding, H.; Long, Y.; Shen, J.; Wan, M. J Phys Chem B 2010, 114, 115.
17. Wang, Y.; Lee, J. Y.; Zeng, H. C. Chem Mater 2005, 17, 3899.
18. Xu, C.; Sun, J.; Gao, L. J Phys Chem C 2009, 113, 20509.
19. Ferrere, S.; Zaban, A.; Gregg, B. A. J Phys Chem B 1997, 101, 4490.
20. Nicholas, C. P.; Marks, T. J. Nano Lett 2004, 4, 1557.
21. Wang, Y. L.; Jiang, X. C.; Xia, Y. N. J Am Chem Soc 2003, 125, 16176.
22. Kolmakov, A.; Zhang, Y. X.; Cheng, G. S.; Moskovits, M. Adv Mater 2003, 15, 997.
23. Huang, J.; Matsunaga, N.; Shimanoe, K.; Yamazoe, N.; Kunitake, T. Chem Mater 2005, 17, 3513.
24. Rajendra Prasad, K.; Miura, N. Electrochem Commun, 2006, 6, 849.
25. Jia, Y.; He, L.; Guo, Z.; Chen, X.; Meng, F.; Luo, T; Li, M.; Liu, J. J Phys Chem C 2009, 113, 9581.
26. Yuan, L.; Wang, J.; Chew, S. Y.; Chen, J.; Guo, Z. P.; Zhao, L.; Konstantinov, K.; Liu, H. K. J Power Sourc 2007, 174, 1183.
27. Kulszewicz-Bajer, I.; Pron, A.; Abramowicz, J.; Jeandey, C.; Oddou, J.-L.; Sobczak, J. W. Chem Mater 1999, 11, 552.
28. Genoud, F.; Kulszewicz-Bajer, I.; Bedel, A.; Oddou, J.-L.; Jeandey, C.; Pron, A. Chem Mater 2000, 12, 744.
29. Tai, H.; Jiangy, Y.; Xie, G.; Yu, J. J Mater Sci Technol 2010, 26, 605.
30. Deshpande, N. G.; Gudage, Y. G.; Sharma, R.; Vyas, J. C.; Kim, J. B.; Lee, Y. P. Sensor Actuator B 2009, 138, 76.
31. Geng, L.; Zhao, Y.; Huang, X.; Wang, S.; Zhang, S.; Wu, S. Sensor Actuator B 2007, 120, 568.
32. Kousik, D.; De. S.K. Materials Letters 2007, 61, 4967.
33. Rajiv, P.; Santhanam, K. S. V. J Solid State Electrochem 1998, 2, 123.
34. Rao, C. R. K.; Trivedi, D. C. Catal Commun 2006, 7, 662.
35. Rao, C. R. K.; Trivedi, D. C. Synthetic Met 2007, 157, 432.
36. Rao, C. R. K.; Vijayan, M. Synthetic Met 2008, 158, 516.
37. Radhakrishnan, S.; Prakash, S.; Rao, C. R. K.; Vijayan, M. Electrochem Solid State Lett 2009, 12, A84.
38. Prakash, S.; Rao, C. R. K.; Vijayan, M. Electrochim Acta 2009, 54, 5919.
39. Trivedi; D. C.; Nalwa, H. S., Eds. Handbook of Organic Conductive Molecules and Polymers, Vol. 2; Wiley: Chichester, England, 1997.
40. Furukawa, Y.; Ueda, F.; Hyoda, Y.; Harada, I.; Nakajima, T.; Kawagoe, T. Macromolecules 1988, B21, 1297.
41. Epstein, A. J.; MacDiarmid, A. G. Mol Cryst Liq Cryst 1988, 160, 165.
42. Sariciftci, N. S.; Kuzmany, H.; Neugebauer, H.; Neckel, A. J Chem Phys 1990, 92, 4530.
43. Li, X. G.; Lu, Q. F.; Huang, M. R. Small 2008, 4, 1201.
44. Moon, Y. B.; Cao, Y.; Smith, P.; Heeger, A. J Polym Commun 1989, 30, 196.
45. Han, W.-Q. Zettl, A. Nano Lett 2003, 3, 681.
46. Shukla, S.; Patil, S.; Kuiry, S. C.; Rahman, Z.; Du, T.; Ludwig, L.; Parish, C.; Seal, S. Sensor Actuator B 2003, 96, 343.
47. Chen, W.; Ghosh, D.; Chen, S. J Mater Sci 2008, 43, 5291.